Majorana lattice gauge theory: symmetry breaking, topological order and intertwined orders all in one

Jian-Jian Miao[1,†]

[1]Department of Physics, The Chinese University of Hong Kong, Shatin, New Territories, Hong Kong, China
Email: [†]jjmiao@phy.cuhk.edu.hk

November 23, 2022

The Majorana lattice gauge theory purely composed of Majorana fermions on square lattice is studied throughly. The ground state is obtained exactly and exhibits the coexistence of symmetry breaking and topological order. The Z_2 symmetry breaking of matter fields leads to the intertwined antiferromagnetic spin order and η-pairing order. The topological order is reflected in the Z_2 quantum spin liquid ground state of gauge fields. The Majorana lattice gauge theory, alternatively can be viewed as interacting Majorana fermion model, is possibly realized on a Majorana-zero-mode lattice.

Introduction

Landau's symmetry breaking theory establishes the first paradigm of phases of matters in condensed matter physics. Different phases are characterized by different symmetries. A phase transition is determined how symmetry changes across the critical point and can be described by the local order parameters that transform nontrivially under the symmetry transformation. Landau's theory successfully accounts for the appearance of various low temperature orders due

to spontaneous symmetry breaking, e.g. crystals and magnets. However, the discovery of fractional quantum Hall (FQH) effect[1] and high-T_c superconductors[2] provides the phenomena beyond the paradigm of Landau's symmetry breaking theory. Anderson proposed the quantum spin liquid[3, 4, 5, 6, 7, 8, 9] (QSL) without symmetry breaking is the key to the mechanism of high-T_c superconductivity[10]. Wen found different chiral spin liquids have exactly the same symmetry[11], as well as different FQH states. These new orders without symmetry breaking and local order parameters are characterized by the topological invariants, e.g. ground state degeneracy on the torus and nontrivial edge states[12]. Dubbed topological orders, these nontrivial gapped disordered phases possess long-range entanglement at zero temperature[13, 14, 15]. A new paradigm of topological phases of matters emerges and flourishes in the past decades[16]. A critical outstanding issue comes that is it possible to unify the symmetry breaking and topological order frameworks into a single formalism?

The Majorana fermion (MF) perspective of strongly correlated systems provide new insights into the issue. The MFs are real counterparts of complex fermions[17, 18, 19]. Not only can be realized experimentally, e.g. in the interface of s-wave superconductor and strong topological insulator[20, 21, 22, 23, 24], but also have the potential to implement topological quantum computation[25], MFs (Majorana zero modes) become the hot topics in condensed matter physics. Moreover the strongly interacting models[26, 27, 28, 29] built from MFs can host exotic phenomena, such as Majorana dualities[30], the emergence of supersymmetry[31, 32, 33] and supersymmetry breaking[34], Majorana surface code[35, 36], tricritical Ising point[37, 38], topological order[39, 40], SYK model with black hole physics[41, 42].

In this paper, a novel Majorana lattice gauge theory is proposed, which can also be viewed as an interacting MF model. The ground state is obtained exactly with matter and gauge fields exhibiting symmetry breaking and topological order respectively. The Z_2 symmetry breaking leads to intertwined antiferromagnetic (AFM) spin and η-pairing orders characterized by local

order parameters. The Z_2 topological order in the Z_2 QSL is characterized by the ground state degeneracy on torus. Even though matter and gauge fields are coupled in the ultraviolet limit, the decoupling of matter and gauge fields in the infrared limit leads to the nontrivial coexistence of symmetry breaking and topological order. The Majorana lattice gauge theory provides the first concrete example to unify symmetry breaking, topological order and intertwined orders.

Results

Majorana lattice gauge theory. The building blocks of Majorana lattice gauge theory are MFs only. The MFs are described by real operators $(\gamma_{\mathbf{r}}^j)^\dagger = \gamma_{\mathbf{r}}^j$ obeying the anticommutation relations $\left\{ \gamma_{\mathbf{r}}^j, \gamma_{\mathbf{r}'}^{j'} \right\} = 2\delta^{jj'}\delta_{\mathbf{rr}'}$ with site index $\mathbf{r}$ and flavor index $j = 1, \cdots, m$. Note the total MF flavors m must be an even integer to ensure locality. For concreteness, a representative gauge theory on square lattice is considered. On each site the matter fields are four γ MFs. The four γ MFs can represent the conventional complex fermion operators $c_{\mathbf{r}s}$ describing the electrons with spin polarization $s = \uparrow, \downarrow$

$$c_{\mathbf{r}\uparrow} = \frac{1}{2} \left(\gamma_{\mathbf{r}}^1 - i\gamma_{\mathbf{r}}^2 \right), \tag{1a}$$

$$c_{\mathbf{r}\downarrow} = \frac{1}{2} \left(\gamma_{\mathbf{r}}^3 - i\gamma_{\mathbf{r}}^4 \right). \tag{1b}$$

The on-site interaction H_U of γ MFs is given by

$$H_U = \frac{U}{4} \sum_{\mathbf{r}} \left(i\gamma_{\mathbf{r}}^1 \gamma_{\mathbf{r}}^2 \right) \left(i\gamma_{\mathbf{r}}^3 \gamma_{\mathbf{r}}^4 \right), \tag{2}$$

$$= U \sum_{\mathbf{r}} \left(n_{\mathbf{r}\uparrow} - \frac{1}{2} \right) \left(n_{\mathbf{r}\downarrow} - \frac{1}{2} \right), \tag{3}$$

where $n_{\mathbf{r}s} = c_{\mathbf{r}s}^\dagger c_{\mathbf{r}s}$ is the electron density operator for spin s. The on-site interaction H_U corresponds to the Hubbard interaction of electrons. Four χ MFs on each site are introduced and act as gauge fields. In the conventional lattice gauge theory, the gauge fields live on the

links of lattice. As shown later, the product of two χ MFs on nearest neighbor sites correspond to the conventional bosonic gauge fields. Thus the total flavors of χ MFs are chosen to be equal to the coordination number $z = 4$ of the square lattice. Besides the on-site interaction H_V with the same form as γ MFs'

$$H_V = V \sum_{\mathbf{r}} \left(i \chi_{\mathbf{r}}^1 \chi_{\mathbf{r}}^2 \right) \left(i \chi_{\mathbf{r}}^3 \chi_{\mathbf{r}}^4 \right), \tag{4}$$

a plaquette interaction H_K of χ MFs is also introduced

$$H_K = K \sum_{\mathbf{r}} \left(i \chi_{\mathbf{r}}^2 \chi_{\mathbf{r}}^1 \right) \left(i \chi_{\mathbf{r}+\hat{x}}^3 \chi_{\mathbf{r}+\hat{x}}^2 \right) \left(i \chi_{\mathbf{r}+\hat{x}+\hat{y}}^4 \chi_{\mathbf{r}+\hat{x}+\hat{y}}^3 \right) \left(i \chi_{\mathbf{r}+\hat{y}}^1 \chi_{\mathbf{r}+\hat{y}}^4 \right) \tag{5}$$

where each term includes four sites forming a plaquette on square lattice. Note all χ Majorana fermions within a plaquette are included in each plaquette interaction as shown in Figure 1, which to pin down the flavor indexes. The square lattice is divided into two dual sublattices a and b, that is the plaquette centers of one sublattice correspond to the sites of another sublattice. The coupling between matter and gauge fields is given by

$$H_t = t \sum_{\langle \mathbf{r}_a \mathbf{r}_b \rangle} \left(i \gamma_{\mathbf{r}_a}^2 \gamma_{\mathbf{r}_b}^1 + i \gamma_{\mathbf{r}_a}^4 \gamma_{\mathbf{r}_b}^3 \right) \left(i \chi_{\mathbf{r}_a}^j \chi_{\mathbf{r}_b}^k \right), \tag{6}$$

$$= t \sum_{\langle \mathbf{r}_a \mathbf{r}_b \rangle s} \left(c_{\mathbf{r}_a s}^\dagger c_{\mathbf{r}_b s} + c_{\mathbf{r}_a s}^\dagger c_{\mathbf{r}_b s}^\dagger + H.c. \right) \left(i \chi_{\mathbf{r}_a}^j \chi_{\mathbf{r}_b}^k \right), \tag{7}$$

where the quadratic γ MFs correspond to nearest neighbor electron hopping and equal-spin-pairing, meanwhile the γ MFs are coupled to χ^j and χ^k MFs connecting nearest neighbor sites as shown in Figure 1. The full Hamiltonian of the Majorana lattice gauge theory is the sum of above interactions

$$H = H_U + H_V + H_K + H_t. \tag{8}$$

which is also an interacting MF model. The Hamiltonian is constructed based on the locality principle, that is interactions are as local as possible. The hidden Z_2 gauge symmetry will be elaborated later. Note the novel Majorana lattice gauge theory is composed of MFs only, which
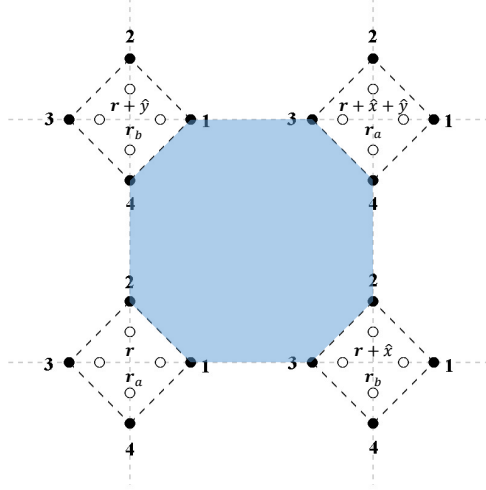
Figure 1: MFs on the square lattice. On each site, four γ and four χ MFs are denoted as white and black points surrounding the site. The numbers $1-4$ denote the MF flavors. The square lattice is divided into two dual sublattices a and b. The shadow region denotes the plaquette interaction H_K.

is different from the conventional gauge theory composed of MFs on sites and spins on links such as [43].

$V = 0$: **exactly solvable model and symmetry breaking of matter fields.** In the limit $V = 0$, the Majorana lattice gauge theory on square lattice reduces to an exactly solvable model $H_0 = H_U + H_K + H_t$. The on-site interaction H_U is obviously composed of commuting projectors, meanwhile the plaquette interaction H_K is also composed of commuting projectors as two neighbor plaquettes share two χ MFs. Note in the coupling H_t, γ^1 and γ^3 on sublattice a meanwhile γ^2 and γ^4 on sublattice b are absent, we define the γ MF *site operators*

$$\hat{C}_{\mathbf{r}} = \begin{cases} i\gamma^1_{\mathbf{r}_a}\gamma^3_{\mathbf{r}_a}, & \mathbf{r} = \mathbf{r}_a \\ i\gamma^2_{\mathbf{r}_b}\gamma^4_{\mathbf{r}_b}. & \mathbf{r} = \mathbf{r}_b \end{cases} \tag{9}$$

Since $\left[\hat{C}_{\mathbf{r}}, H_0\right] = 0$, the site operators are constants of motion in the limit $V = 0$. Also $\hat{C}_{\mathbf{r}}^2 = 1$,

the eigenvalues of the site operators take Z_2 values $C_{\mathbf{r}} = \pm 1$. The on-site interaction H_U can be written in terms of site operators as

$$H_U = -\frac{U}{4} \left[\sum_{\mathbf{r}_a} \hat{C}_{\mathbf{r}_a} \left(i\gamma^2_{\mathbf{r}_a} \gamma^4_{\mathbf{r}_a} \right) + \sum_{\mathbf{r}_b} \hat{C}_{\mathbf{r}_b} \left(i\gamma^1_{\mathbf{r}_b} \gamma^3_{\mathbf{r}_b} \right) \right]. \tag{10}$$

Similarly we define the χ MF *bond operators*

$$\hat{D}_{\mathbf{r},\mathbf{r}'} = -\hat{D}_{\mathbf{r}',\mathbf{r}} = \begin{cases} i\chi^1_{\mathbf{r}} \chi^3_{\mathbf{r}'}, & \mathbf{r}' = \mathbf{r} + \hat{x} \\ i\chi^2_{\mathbf{r}} \chi^4_{\mathbf{r}'}. & \mathbf{r}' = \mathbf{r} + \hat{y} \end{cases} \tag{11}$$

As $\left[\hat{D}_{\mathbf{r},\mathbf{r}'}, H_0 \right] = 0$ and $\hat{D}^2_{\mathbf{r},\mathbf{r}'} = 1$, the bond operators are also constants of motion in the limit $V = 0$ with Z_2 eigenvalues $D_{\mathbf{r},\mathbf{r}'} = \pm 1$. The plaquette interaction H_K and coupling H_t can be written in terms of bond operators as

$$H_K = -K \sum_{\mathbf{r}} \hat{D}_{\mathbf{r},\mathbf{r}+\hat{x}} \hat{D}_{\mathbf{r}+\hat{x},\mathbf{r}+\hat{x}+\hat{y}} \hat{D}_{\mathbf{r}+\hat{x}+\hat{y},\mathbf{r}+\hat{y}} \hat{D}_{\mathbf{r}+\hat{y},\mathbf{r}}, \tag{12}$$

$$H_t = t \sum_{\langle \mathbf{r}_a \mathbf{r}_b \rangle} \left(i\gamma^2_{\mathbf{r}_a} \gamma^1_{\mathbf{r}_b} + i\gamma^4_{\mathbf{r}_a} \gamma^3_{\mathbf{r}_b} \right) \hat{D}_{\mathbf{r}_a,\mathbf{r}_b}. \tag{13}$$

Therefore in the limit $V = 0$ the Majorana lattice gauge theory reduces to the quadratic γ MFs coupled to the static Z_2 gauge fields. The constants of motion $\hat{C}_{\mathbf{r}}$ and $\hat{D}_{\mathbf{r},\mathbf{r}'}$ serve as static Z_2 gauge fields. The exact solvability of the model H_0 is in the same spirit of the exactly solvable Kitaev honeycomb model[44].

We can replace the operators $\hat{C}_{\mathbf{r}}$ and $\hat{D}_{\mathbf{r},\mathbf{r}'}$ by their eigenvalues in H_0 and the ground states of H_0 is determined by the configurations $\{C_{\mathbf{r}}\}$ and $\{D_{\mathbf{r},\mathbf{r}'}\}$ with lowest energy. The plaquette interaction H_K is of the same form of Wegner's Ising lattice gauge theory[45], where the Z_2 eigenvalues $D_{\mathbf{r},\mathbf{r}'} = \pm 1$ act as classical Ising spins. We define the *local gauge transformation* $G_{\mathbf{r}}$ on site $\mathbf{r}$ that only the $D_{\mathbf{r},\mathbf{r}'}$ connecting to site $\mathbf{r}$ change sign

$$G_{\mathbf{r}} : D_{\mathbf{r},\mathbf{r}'} \to -D_{\mathbf{r},\mathbf{r}'}, \tag{14a}$$

meanwhile the γ MFs on site $\mathbf{r}$ change as

$$\begin{cases} \gamma^2_{\mathbf{r}_a} \to -\gamma^2_{\mathbf{r}_a}, \ \gamma^4_{\mathbf{r}_a} \to -\gamma^4_{\mathbf{r}_a}, & \mathbf{r} = \mathbf{r}_a \\ \gamma^1_{\mathbf{r}_b} \to -\gamma^1_{\mathbf{r}_b}, \ \gamma^3_{\mathbf{r}_b} \to -\gamma^3_{\mathbf{r}_b}. & \mathbf{r} = \mathbf{r}_b \end{cases} \tag{14b}$$

which is the hidden Z_2 gauge symmetry even for $V \neq 0$. The Hamiltonian H_0 is gauge invariant, thus the ground state configurations $\{D_{\mathbf{r},\mathbf{r}'}\}$ include 2^N configurations that can be related to the uniform configuration $\{D_{\mathbf{r},\mathbf{r}'} = 1\}$[46] by all local gauge transformations, where N is the total number of sites, i.e. the total number of local gauge transformations. Note the local gauge transformations won't alter the γ MF site operators. To determine the ground state configurations $\{C_{\mathbf{r}}\}$, the positive large-U limit is firstly considered to gain intuitive physical understanding. The positive large-U limit enforces the two low-energy states of γ MFs on each site as $i\gamma_{\mathbf{r}_a}^2 \gamma_{\mathbf{r}_a}^4 = C_{\mathbf{r}_a} = \pm 1$ if site belongs to a sublattice or $i\gamma_{\mathbf{r}_b}^1 \gamma_{\mathbf{r}_b}^3 = C_{\mathbf{r}_b} = \pm 1$ if site belongs to b sublattice. Thus the ground state configurations $\{C_{\mathbf{r}}\}$ must be within the low-energy subspace of 2^N direct product states. In the limit $U \gg |t|$, the coupling H_t can be treated as perturbation and the perturbation theory is adopted to derive the effective Hamiltonian within the low-energy subspace

$$H^{\text{eff}} = -\frac{t^2}{U} \sum_{\langle \mathbf{r}_a \mathbf{r}_b \rangle} \left(i\gamma_{\mathbf{r}_a}^2 \gamma_{\mathbf{r}_b}^1 \right) \left(i\gamma_{\mathbf{r}_a}^4 \gamma_{\mathbf{r}_b}^3 \right) \hat{D}_{\mathbf{r}_a,\mathbf{r}_b}^2 = \frac{t^2}{U} \sum_{\langle \mathbf{r}_a \mathbf{r}_b \rangle} C_{\mathbf{r}_a} C_{\mathbf{r}_b}, \tag{15}$$

where only even orders survive and the lowest nontrivial terms come from second order. The effective Hamiltonian is the AFM Ising model. Note even the γ MFs and χ MF bond operators are coupled in the ultraviolet limit, the effective Hamiltonian is independent of bond operators. Thus the γ and χ MFs are deoupled in the infrared limit due to the Z_2 characteristic of bond operators. The AFM Ising model indicates the ground state configurations are $\{C_{\mathbf{r}_a} = -C_{\mathbf{r}_b} = \pm 1\}$ with two-fold degeneracy in the positive large-U limit and high order terms won't lift the degeneracy. For generic interaction strength U, the ground state configurations $\{C_{\mathbf{r}}\}$ can be determined numerically by diagonalizing the quadratic γ MFs on finite size lattice and searching for the configurations with lowest ground state energy. The two-fold degeneracy of ground state configurations $\{C_{\mathbf{r}_a} = -C_{\mathbf{r}_b} = \pm 1\}$ is confirmed even for small and negative U. Once the ground state configurations are pinned down, the orders in the ground

states can be identified.

The two-fold degeneracy in terms of γ MF site operators indicates the Z_2 symmetry breaking of matter fields in the ground states of of H_0. There exists a global Z_2 symmetry of the full Hamiltonian H by interchanging γ MFs as follows

$$\gamma_{\mathbf{r}}^1 \leftrightarrow \gamma_{\mathbf{r}}^3, \tag{16a}$$

$$\gamma_{\mathbf{r}}^2 \leftrightarrow \gamma_{\mathbf{r}}^4. \tag{16b}$$

meanwhile the site operators change sign $\hat{C}_{\mathbf{r}} \leftrightarrow -\hat{C}_{\mathbf{r}}$ under Z_2 symmetry transformation. Thus the expectation values of $\hat{C}_{\mathbf{r}}$ naturally serve as local order parameters. Nevertheless we shall define more physical local order parameters in terms of electron operators by introducing the spin and charge operators

$$\hat{S}_{\mathbf{r}}^\alpha = \frac{1}{2} \left(\begin{array}{cc} c_{\mathbf{r}\uparrow}^\dagger & c_{\mathbf{r}\downarrow}^\dagger \end{array} \right) \tau^\alpha \left(\begin{array}{c} c_{\mathbf{r}\uparrow} \\ c_{\mathbf{r}\downarrow} \end{array} \right), \tag{17}$$

$$\hat{Q}_{\mathbf{r}}^\alpha = \frac{1}{2} \left(\begin{array}{cc} c_{\mathbf{r}\uparrow}^\dagger & c_{\mathbf{r}\downarrow} \end{array} \right) \tau^\alpha \left(\begin{array}{c} c_{\mathbf{r}\uparrow} \\ c_{\mathbf{r}\downarrow}^\dagger \end{array} \right), \tag{18}$$

where τ^α are Pauli matrices with $\alpha = x, y, z$. Note the operator $2\hat{Q}_{\mathbf{r}}^z = n_{\mathbf{r}\uparrow} + n_{\mathbf{r}\downarrow} - 1$ measures the charges with respect to half-filling. Since

$$\hat{S}_{\mathbf{r}_a}^y + \hat{Q}_{\mathbf{r}_a}^y = -\frac{1}{2} \hat{C}_{\mathbf{r}_a}, \tag{19}$$

$$\hat{S}_{\mathbf{r}_b}^y - \hat{Q}_{\mathbf{r}_b}^y = -\frac{1}{2} \hat{C}_{\mathbf{r}_b}, \tag{20}$$

the y-components of spin and charge operators also transform nontrivially under Z_2 symmetry transformation and the their expectation values $S_{\mathbf{r}}^y = \left\langle \hat{S}_{\mathbf{r}}^y \right\rangle$ and $Q_{\mathbf{r}}^y = \left\langle \hat{Q}_{\mathbf{r}}^y \right\rangle$ serve as local order parameters. Without loss of generality, the local order parameters are calculated under the uniform configuration $\{D_{\mathbf{r},\mathbf{r}'} = 1\}$ which differs other configurations by local gauge transformation. In the uniform configuration the model H_0 is equivalent to the BCS-Hubbard model
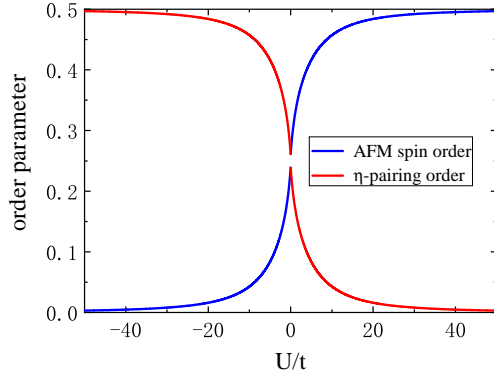
Figure 2: The magnitudes of local order parameters $|S_{\mathbf{r}}^y|$ and $|Q_{\mathbf{r}}^y|$ as function of U/t. The singular point $U = 0$ indicates the gap close of E_k. In the large positive/negative U limit, the magnitude of spin/pairing order saturates.

at the exactly solvable point[47], and the local order parameters are given by

$$S_{\mathbf{r}}^y = \pm (-)^{\mathbf{r}} \frac{1}{4} \left(1 + \frac{1}{N} \sideset{}{'}\sum_{\mathbf{k}} \frac{U}{E_k} \right), \tag{21}$$

$$Q_{\mathbf{r}}^y = \pm \frac{1}{4} \left(1 - \frac{1}{N} \sideset{}{'}\sum_{\mathbf{k}} \frac{U}{E_k} \right), \tag{22}$$

where $E_k = \frac{1}{2}\sqrt{U^2 + 16t^2 \epsilon_{\mathbf{k}}^2}$ is the quasiparticle dispersion of γ MFs and $\epsilon_{\mathbf{k}} = 2 \left(\cos k_x + \cos k_y \right)$ is the form factor on square lattice. The summation $\sideset{}{'}\sum_{\mathbf{k}}$ is over the folded Brillouin zone. $S_{\mathbf{r}}^y$ and $Q_{\mathbf{r}}^y$ characterize the spin and pairing orders respectively. The staggered factor in $S_{\mathbf{r}}^y$ indicates the spin order is the AFM order. Recall the definition $Q_{\mathbf{r}}^y = \frac{i}{2} \left\langle c_{\mathbf{r}\downarrow}c_{\mathbf{r}\uparrow} - c_{\mathbf{r}\uparrow}^\dagger c_{\mathbf{r}\downarrow}^\dagger \right\rangle$, the pairing order is the spin-singlet η-pairing[48, 49]. The two orders coexist as they break the same Z_2 symmetry. However the repulsive Hubbard interaction favors the spin order while the attractive Hubbard interaction favors the pairing order. Thus the two orders also compete with each other that lead to the waxing and waning pattern of magnitudes of local order parameters in Figure. 2. Such coexistence and competition of orders in an exactly solvable model provide a concrete example of intertwined orders in strongly correlated electron systems[50].

$V \neq 0$: **exact ground state and topological order of gauge fields.** The on-site interaction H_V spoils the exact solvability of H_0 as $\left\{ \left(i\chi_{\mathbf{r}}^1 \chi_{\mathbf{r}}^2 \right) \left(i\chi_{\mathbf{r}}^3 \chi_{\mathbf{r}}^4 \right), \hat{D}_{\mathbf{r},\mathbf{r}'} \right\} = 0$. To gain intuitive understanding of physical effect of H_V, the large-V limit is firstly considered. As $\left(\chi_{\mathbf{r}}^1 \chi_{\mathbf{r}}^2 \chi_{\mathbf{r}}^3 \chi_{\mathbf{r}}^4 \right)^2 = 1$, in the limit $|V| \gg |K|$ the two low-energy states of χ MFs on each site are identified as $\chi_{\mathbf{r}}^1 \chi_{\mathbf{r}}^2 \chi_{\mathbf{r}}^3 \chi_{\mathbf{r}}^4 = \mathrm{sign}V$, where $\mathrm{sign}V$ is the sign of on-site interaction strength V. Thus the on-site interaction H_V can be viewed as local constraints in the large-V limit. We define the Pauli spin operators in terms of χ MFs

$$\sigma_{\mathbf{r}}^x = i\chi_{\mathbf{r}}^1 \chi_{\mathbf{r}}^2 = \mathrm{sign}V i\chi_{\mathbf{r}}^4 \chi_{\mathbf{r}}^3, \tag{23a}$$

$$\sigma_{\mathbf{r}}^y = i\chi_{\mathbf{r}}^1 \chi_{\mathbf{r}}^3 = \mathrm{sign}V i\chi_{\mathbf{r}}^2 \chi_{\mathbf{r}}^4, \tag{23b}$$

$$\sigma_{\mathbf{r}}^z = \mathrm{sign}V i\chi_{\mathbf{r}}^1 \chi_{\mathbf{r}}^4 = i\chi_{\mathbf{r}}^3 \chi_{\mathbf{r}}^2, \tag{23c}$$

where the local constraints $\chi_{\mathbf{r}}^1 \chi_{\mathbf{r}}^2 \chi_{\mathbf{r}}^3 \chi_{\mathbf{r}}^4 = \mathrm{sign}V$ are used in the second equality. The four χ MFs with local constraints give a faithful representation of Pauli spin operators, such as the identity $\sigma_{\mathbf{r}}^x \sigma_{\mathbf{r}}^y \sigma_{\mathbf{r}}^z = \mathrm{sign}V i\chi_{\mathbf{r}}^1 \chi_{\mathbf{r}}^2 \chi_{\mathbf{r}}^3 \chi_{\mathbf{r}}^4 = i$, and the two low-energy states on each site also match the two-dimensional Hilbert space of Pauli spin. The plaquette interaction H_K in the Pauli spin representation is given by

$$H_K = -K \left(\mathrm{sign}V \right)^2 \sum_{\mathbf{r}} \sigma_{\mathbf{r}}^x \sigma_{\mathbf{r}+\hat{x}}^z \sigma_{\mathbf{r}+\hat{x}+\hat{y}}^x \sigma_{\mathbf{r}+\hat{y}}^z, \tag{24}$$

which is the exactly solvable Wen plaquette model[51], and is equivalent to the toric code[52] hosting the exact Z_2 QSL ground state with topological order. The ground states of Wen plaquette model on torus is topologically four-fold degeneracy. Note different $\mathrm{sign}V$'s lead to the same topological order.

In the spirit of Noether's theorem, the local gauge symmetry has a corresponding conserved gauge charge and vice versa. Thus the Z_2 gauge symmetry in Eq. 14 leads to the conservation of Z_2 gauge charge $\hat{P}_{\mathbf{r}} = \hat{M}_{\mathbf{r}} \hat{G}_{\mathbf{r}}$, where $\hat{M}_{\mathbf{r}} = \gamma_{\mathbf{r}}^1 \gamma_{\mathbf{r}}^2 \gamma_{\mathbf{r}}^3 \gamma_{\mathbf{r}}^4$ and $\hat{G}_{\mathbf{r}} = \chi_{\mathbf{r}}^1 \chi_{\mathbf{r}}^2 \chi_{\mathbf{r}}^3 \chi_{\mathbf{r}}^4$ characterize the

fermion number parities of γ and χ MFs on each site respectively. The properties $\left[H, \hat{P}_{\mathbf{r}}\right] = 0$ and $\hat{P}_{\mathbf{r}}^2 = 1$ manifest the Z_2 characteristic of conserved gauge charge $P_{\mathbf{r}} = \pm 1$. Even though separate fermion number parities of γ and χ MFs are not conserved due to the coupling H_t, their total fermion number parity $P_{\mathbf{r}}$ is conserved in the ultraviolet limit. In $V \neq 0$ the site operators are still constants of motion but the bond operators are not. In the eigenbasis of bond operators, the signs $D_{\mathbf{r},\mathbf{r}'} = \pm 1$ in the coupling H_t in Eq. 13 can be absorbed by the local gauge transformation. Thus the physics of γ MFs, that is symmetry breaking and intertwined orders of matter fields, is unchanged in $V \neq 0$. Moreover, as shown in the limit $U \gg |t|$ in Eq. 15 the γ and χ MFs are explicitly decoupled in the infrared limit due to $\hat{D}_{\mathbf{r},\mathbf{r}'}^2 = 1$. The low-energy effective Hamiltonian of gauge fields can be captured by $H_K + H_V$[53]. In the small-V limit $|V| \ll |K|$, the ground state of gauge fields must lie in the 2^N ground state configurations of plaquette interaction H_K. The 2^N configurations are related to the uniform configuration $\{D_{\mathbf{r},\mathbf{r}'} = 1\}$ by all local gauge transformations. Note the operators $\hat{G}_{\mathbf{r}} = \chi_{\mathbf{r}}^1 \chi_{\mathbf{r}}^2 \chi_{\mathbf{r}}^3 \chi_{\mathbf{r}}^4$ constituting the on-site interaction H_V implements the local gauge transformation $G_{\mathbf{r}}$ in Eq. 14. Thus the ground state of gauge fields is the equal weight linear superposition of 2^N gauge equivalent configurations, which is the famous Anderson's resonating valence bond state of QSL[3, 10]. In the ground state $\hat{G}_{\mathbf{r}} = \chi_{\mathbf{r}}^1 \chi_{\mathbf{r}}^2 \chi_{\mathbf{r}}^3 \chi_{\mathbf{r}}^4 = 1$, which is identical to the local constraint in the limit $|V| \gg |K|$ wherein the sign$V$ is irrelevant to ground state. The QSL ground state in the small-V limit is adiabatically connected to the Z_2 QSL ground state in the large-V limit. Even though the exact solvability of H_0 is spoiled by on-site interaction H_V, the exact ground state of H is still extracted. The conservation of fermion number parity $\hat{G}_{\mathbf{r}} = 1$ of χ MFs in the exact ground state is another manifestation of decoupling of matter and gauge fields in the infrared limit. The conserved Z_2 gauge charge $\hat{G}_{\mathbf{r}} = 1$ corresponds to the local gauge symmetry of gauge fields only.

The zero-temperature phase diagram of Majorana lattice gauge theory for $V \neq 0$ is sketched
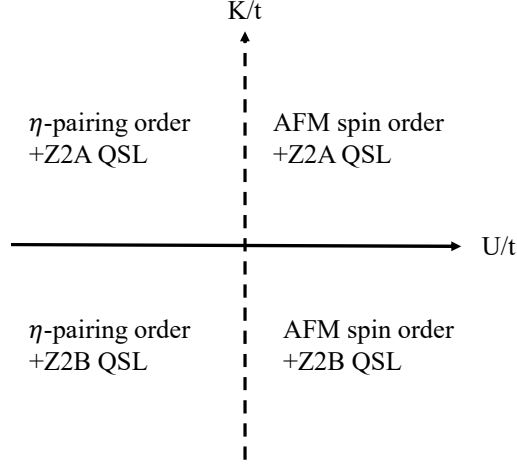
Figure 3: Zero-temperature phase diagram of Majorana lattice gauge theory for $V \neq 0$. The dashed line $U/t = 0$ denotes a crossover. The solid line $K/t = 0$ denotes a topological phase transition.

in Figure. 3. Besides the irrelevance of $\mathrm{sign}V$, the sign of coupling constant t is also irrelevant to ground state due to the bipartiteness of square lattice and we set $t > 0$. In regards of matter fields, the AFM spin order dominates for positive U, while the η-pairing order dominates for negative U. The singular point $U = 0$ indicates the macroscopic degeneracy due to all local constants of motion, i.e. all site operators, but not a critical point. The separation line $U/t = 0$ in the phase diagram is not phase boundary but only a crossover. As for gauge fields, the ground state is $Z2A$ and $Z2B$ QSL for positive and negative K respectively, which terminology is from the projective symmetry group classification[51]. The essential difference between $Z2A$ and $Z2B$ QSL is the Z_2 flux $F_{\mathbf{r}} = \sigma^x_{\mathbf{r}} \sigma^z_{\mathbf{r}+\hat{x}} \sigma^x_{\mathbf{r}+\hat{x}+\hat{y}} \sigma^z_{\mathbf{r}+\hat{y}} = \pm 1$ constituting the plaquette interaction H_K in Eq. 24. The phase transition line $K/t = 0$ corresponds to topological phase transition.

Discussion

The Majorana lattice gauge theory with γ and χ MFs act as matter and gauge fields respectively on square lattice is studied throughly. The matter fields with symmetry breaking exhibit intertwined AFM spin order and η-pairing order, both of which break the same Z_2 symmetry meanwhile compete with each other. The gauge fields form Z_2 QSL ground state with Z_2 topological order therein. The unexpected coexistence of symmetry breaking and topological order is due to the decoupling of matter and gauge fields in the infrared limit, which is unique to Majorana/Z_2 lattice gauge theory and can't be straightforwardly generalized to other lattice gauge theories with discrete Z_N ($N > 2$) or continuous symmetries. Formally, the global symmetry of matter fields can be spontaneously broken that leads to local order parameters. However the local gauge symmetry of gauge fields can never be broken according to Elitzur theorem[54, 55] but can host topological order. The Majorana lattice gauge theory can unify these two frameworks in a single formalism.

The Majorana lattice gauge theory on square lattice is equivalent to Wegner's Ising gauge theory, AFM Ising model, BCS-Hubbard model, Wen plaquette model and toric code in various limits. On the other hand, Majorana lattice gauge theory can be easily generalized to other lattices and higher dimensions. Simply let the number of χ MFs on each site equals to the site coordination number z. We can also introduce $2m$ γ MFs with $m > 2$ to include more degrees of freedom besides charge and spin, e.g. orbit. In principle the Majorana lattice gauge theory can harbor more exotic coexistence of different symmetry breaking and topological order.

The Majorana lattice gauge theory purely composed of MFs can be alternatively viewed as an interacting MF model. Recently, the Majorana-zero-mode lattice has been realized in a tunable way[56], which provides a natural platform to implement interacting MF model composed of local interactions only. Experimentally, the Z_2 domain wall as symmetry defect of Z_2

symmetry breaking can be detected by local probe, e.g. STM. Theoretically, the topological order is reflected in the ground state degeneracy on nontrivial base manifold[57]. A more realistic scheme is the detection of vison excitation of Z_2 topological order[58]. Future direction of research is the doping effect, that is doping on γ or χ MFs to study the effect on AFM spin order or QSL, which may provide clues to high-T_c cuprates.

Acknowledgement

JJM is grateful for the suggestions and comments from Yi Zhou. This work is supported by General Research Fund Grant No. 14302021 from Research Grants Council and Direct Grant No. 4053416 from the Chinese University of Hong Kong.

References

[1] Tsui, D. C., Stormer, H. L., Gossard, A. C. (1982). Two-dimensional magnetotransport in the extreme quantum limit. Physical Review Letters, 48(22), 1559.

[2] Bednorz, J. G., Muller, K. A. (1986). Possible highT c superconductivity in the Ba-La-Cu-O system. Zeitschrift fur Physik B Condensed Matter, 64(2), 189-193.

[3] Anderson, P. W. (1973). Resonating valence bonds: A new kind of insulator?. Materials Research Bulletin, 8(2), 153-160.

[4] Lee, P. A. (2008). An end to the drought of quantum spin liquids. Science, 321(5894), 1306-1307.

[5] Balents, L. (2010). Spin liquids in frustrated magnets. Nature, 464(7286), 199-208.

[6] Savary, L., Balents, L. (2016). Quantum spin liquids: a review. Reports on Progress in Physics, 80(1), 016502.

[7] Zhou, Y., Kanoda, K., Ng, T. K. (2017). Quantum spin liquid states. Reviews of Modern Physics, 89(2), 025003.

[8] Knolle, J., Moessner, R. (2019). A Field Guide to Spin Liquids. Annual Review of Condensed Matter Physics, 10, 451-472.

[9] Broholm, C., Cava, R. J., Kivelson, S. A., Nocera, D. G., Norman, M. R. (2020). T. Senthil. Quantum spin liquids. Science, 367, 263.

[10] Anderson, P. W. (1987). The resonating valence bond state in La2CuO4 and superconductivity. science, 235(4793), 1196-1198.

[11] Wen, X. G. (1989). Vacuum degeneracy of chiral spin states in compactified space. Physical Review B, 40(10), 7387.

[12] Wen, X. G. (1990). Topological orders in rigid states. International Journal of Modern Physics B, 4(02), 239-271.

[13] Kitaev, A., Preskill, J. (2006). Topological entanglement entropy. Physical review letters, 96(11), 110404.

[14] Levin, M., Wen, X. G. (2006). Detecting topological order in a ground state wave function. Physical review letters, 96(11), 110405.

[15] Chen, X., Gu, Z. C., Wen, X. G. (2010). Local unitary transformation, long-range quantum entanglement, wave function renormalization, and topological order. Physical review b, 82(15), 155138.

[16] Wen, X. G. (2017). Colloquium: Zoo of quantum-topological phases of matter. Reviews of Modern Physics, 89(4), 041004.

[17] Alicea, J. (2012). New directions in the pursuit of Majorana fermions in solid state systems. Reports on progress in physics, 75(7), 076501.

[18] Beenakker, C. W. J. (2013). Search for Majorana Fermions in Superconductors. Annu. Rev. Condens. Matter Phys., 4(1), 113-136.

[19] Elliott, S. R., Franz, M. (2015). Colloquium: Majorana fermions in nuclear, particle, and solid-state physics. Reviews of Modern Physics, 87(1), 137.

[20] Fu, L., Kane, C. L. (2008). Superconducting proximity effect and Majorana fermions at the surface of a topological insulator. Physical review letters, 100(9), 096407.

[21] Sau, J. D., Lutchyn, R. M., Tewari, S., Sarma, S. D. (2010). Generic new platform for topological quantum computation using semiconductor heterostructures. Physical review letters, 104(4), 040502.

[22] Alicea, J. (2010). Majorana fermions in a tunable semiconductor device. Physical Review B, 81(12), 125318.

[23] Lutchyn, R. M., Sau, J. D., Sarma, S. D. (2010). Majorana fermions and a topological phase transition in semiconductor-superconductor heterostructures. Physical review letters, 105(7), 077001.

[24] Oreg, Y., Refael, G., Von Oppen, F. (2010). Helical liquids and Majorana bound states in quantum wires. Physical review letters, 105(17), 177002.

[25] Nayak, C., Simon, S. H., Stern, A., Freedman, M., Sarma, S. D. (2008). Non-Abelian anyons and topological quantum computation. Reviews of Modern Physics, 80(3), 1083.

[26] Chiu, C. K., Pikulin, D. I., Franz, M. (2015). Strongly interacting Majorana fermions. Physical Review B, 91(16), 165402.

[27] Rahmani, A., Pikulin, D., Affleck, I. (2019). Phase diagrams of Majorana-Hubbard ladders. Physical Review B, 99(8), 085110.

[28] Affleck, I., Rahmani, A., Pikulin, D. (2017). Majorana-Hubbard model on the square lattice. Physical Review B, 96(12), 125121.

[29] Rahmani, A., Franz, M. (2019). Interacting majorana fermions. Reports on Progress in Physics, 82(8), 084501.

[30] Nussinov, Z., Ortiz, G., Cobanera, E. (2012). Arbitrary dimensional Majorana dualities and architectures for topological matter. Physical Review B, 86(8), 085415.

[31] Grover, T., Sheng, D. N., Vishwanath, A. (2014). Emergent space-time supersymmetry at the boundary of a topological phase. Science, 344(6181), 280-283.

[32] Rahmani, A., Zhu, X., Franz, M., Affleck, I. (2015). Emergent supersymmetry from strongly interacting Majorana zero modes. Physical review letters, 115(16), 166401.

[33] Rahmani, A., Zhu, X., Franz, M., Affleck, I. (2015). Phase diagram of the interacting Majorana chain model. Physical Review B, 92(23), 235123.

[34] Sannomiya, N., Katsura, H. (2019). Supersymmetry breaking and Nambu-Goldstone fermions in interacting Majorana chains. Physical Review D, 99(4), 045002.

[35] Vijay, S., Hsieh, T. H., Fu, L. (2015). Majorana fermion surface code for universal quantum computation. Physical Review X, 5(4), 041038.

[36] Landau, L. A., Plugge, S., Sela, E., Altland, A., Albrecht, S. M., Egger, R. (2016). Towards realistic implementations of a Majorana surface code. Physical review letters, 116(5), 050501.

[37] Zhu, X., Franz, M. (2016). Tricritical Ising phase transition in a two-ladder Majorana fermion lattice. Physical Review B, 93(19), 195118.

[38] O'Brien, E., Fendley, P. (2018). Lattice supersymmetry and order-disorder coexistence in the tricritical Ising model. Physical review letters, 120(20), 206403.

[39] Katsura, H., Schuricht, D., Takahashi, M. (2015). Exact ground states and topological order in interacting Kitaev/Majorana chains. Physical Review B, 92(11), 115137.

[40] Miao, J. J., Jin, H. K., Zhang, F. C., Zhou, Y. (2017). Exact solution for the interacting Kitaev chain at the symmetric point. Physical Review Letters, 118(26), 267701.

[41] Sachdev, S., Ye, J. (1993). Gapless spin-fluid ground state in a random quantum Heisenberg magnet. Physical review letters, 70(21), 3339.

[42] Kitaev A 2015 KITP Strings Seminar and Entanglement 2015 Program (http://online.kitp.ucsb.edu/online/ entangled15/)

[43] Prosko, C., Lee, S. P., Maciejko, J. (2017). Simple Z 2 lattice gauge theories at finite fermion density. Physical Review B, 96(20), 205104

[44] Kitaev, A. (2006). Anyons in an exactly solved model and beyond. Annals of Physics, 321(1), 2-111.

[45] Wegner, F. J. (1971). Duality in generalized Ising models and phase transitions without local order parameters. Journal of Mathematical Physics, 12(10), 2259-2272.

[46] For positive K, the representative ground state configuration is uniform configuration. For negative K, the representative ground state configuration is $\{D_{\mathbf{r}_a,\mathbf{r}_a+\hat{x}} = -1, D_{\mathbf{r}_b,\mathbf{r}_b+\hat{x}} = D_{\mathbf{r},\mathbf{r}+\hat{y}} = 1\}$.

[47] Chen, Z., Li, X., Ng, T. K. (2018). Exactly solvable bcs-hubbard model in arbitrary dimensions. Physical Review Letters, 120(4), 046401.

[48] Yang, C. N. (1989). η pairing and off-diagonal long-range order in a Hubbard model. Physical review letters, 63(19), 2144.

[49] Yang, C. N., Zhang, S. C. (1990). SO (4) symmetry in a Hubbard model. Modern Physics Letters B, 4(11), 759-766.

[50] Fradkin, E., Kivelson, S. A., Tranquada, J. M. (2015). Colloquium: Theory of intertwined orders in high temperature superconductors. Reviews of Modern Physics, 87(2), 457.

[51] Wen, X. G. (2003). Quantum orders in an exact soluble model. Physical review letters, 90(1), 016803.

[52] Kitaev, A. Y. (2003). Fault-tolerant quantum computation by anyons. Annals of Physics, 303(1), 2-30.

[53] In principle, the matter fields can be integrated to derive the effective Hamiltonian of gauge fields. The coupling H_t will generate effective interaction of bond operators. The local gauge symmetry $G_{\mathbf{r}}$ requires the bond operators in effective interaction form closed loop. The most dominant effective interaction is just the plaquette interaction H_K.

[54] Elitzur, S. (1975). Impossibility of spontaneously breaking local symmetries. Physical review d, 12(12), 3978.

[55] Kogut, J. B. (1979). An introduction to lattice gauge theory and spin systems. Reviews of Modern Physics, 51(4), 659.

[56] Li, M., Li, G., Cao, L., Zhou, X., Wang, X., Jin, C., Chiu, C. K., Pennycook, S. J., Wang, Z., Gao, H. J. (2022). Ordered and tunable Majorana-zero-mode lattice in naturally strained LiFeAs. Nature, 1-6.

[57] Wen, X. G., Niu, Q. (1990). Ground-state degeneracy of the fractional quantum Hall states in the presence of a random potential and on high-genus Riemann surfaces. Physical Review B, 41(13), 9377.

[58] Senthil, T., Fisher, M. P. (2001). Fractionalization in the cuprates Detecting the topological order. Physical review letters, 86(2), 292